NASA TECHNICAL NOTE

NASA TN D-5612

c. 1

NASA TN D-5612

FORCED-CONVECTION BOILING NEAR INCEPTION IN ZERO GRAVITY

by Thomas H. Cochran

Lewis Research Center
Cleveland, Ohio

NATIONAL AERONAUTICS AND SPACE ADMINISTRATION • WASHINGTON, D. C. • JANUARY 1970

1. Report No. NASA TN D-5612	2. Government Accession No.	3. Recipient's Catalog No.
4. Title and Subtitle FORCED-CONVECTION BOILING NEAR INCEPTION IN ZERO GRAVITY		5. Report Date January 1970 6. Performing Organization Code
7. Author(s) Thomas H. Cochran		8. Performing Organization Report No. E-5148
9. Performing Organization Name and Address Lewis Research Center National Aeronautics and Space Administration Cleveland, Ohio 44135		10. Work Unit No. 124-09 11. Contract or Grant No. 13. Type of Report and Period Covered Technical Note
12. Sponsoring Agency Name and Address National Aeronautics and Space Administration Washington, D.C. 20546		14. Sponsoring Agency Code
15. Supplementary Notes		

16. Abstract

An experimental program was conducted to study the behavior of forced-convection boiling at low heat flux and low flow velocities in zero gravity for slightly subcooled distilled water. The results indicated the existence of a bubble boundary layer on the heated surface. A correlation for the size of the bubbles was obtained and found to be a function of the saturation layer thickness.

17. Key Words (Suggested by Author(s)) Forced convection Boiling Zero gravity	18. Distribution Statement Unclassified - unlimited		
19. Security Classif. (of this report) Unclassified	20. Security Classif. (of this page) Unclassified	21. No. of Pages 24	22. Price* $3.00

*For sale by the Clearinghouse for Federal Scientific and Technical Information Springfield, Virginia 22151

FORCED-CONVECTION BOILING NEAR INCEPTION IN ZERO GRAVITY

by Thomas H. Cochran

Lewis Research Center

SUMMARY

An experimental program was conducted to study the behavior of forced-convection boiling in zero gravity. The tests were conducted at the NASA Lewis Research Center Drop Tower Facility. Heat fluxes were near the inception point of boiling, and bulk temperatures were slightly below saturation. The free-stream velocity, which was the primary test variable, was of the same order of magnitude as free-convection velocity for the heater geometry in normal gravity. The results indicated the existence of a bubble boundary layer on the heated surface. A correlation for the size of the bubbles was obtained and found to be a function of the saturation layer thickness.

INTRODUCTION

Cryogenic fluids are one type of propellant that is used in present day spacecraft. The primary advantage in using cryogens is the characteristic high specific impulse they produce. A disadvantage is their low equilibrium temperature that can result in net heat addition, vapor generation, and a corresponding rise in the tank pressure (ref. 1). For some launch vehicles, this disadvantage is not a serious problem because of the relatively short storage times involved and the positive accelerations to which they are subjected. The positive accelerations permit prediction of the location of the liquid-vapor interface and, hence, enable tank pressure to be lowered by venting vapor. In long-term space flights, however, the rocket may be subjected to zero- or low-gravity environments so that the interface cannot be accurately located. Venting under these conditions could result in the loss of liquid propellant.

One method that has been proposed to resolve the pressure rise problem for this situation is termed the thermal conditioning system (ref. 2). The basic concept of the thermal conditioning system is to remove propellant from a tank, expand it to a lower temperature and pressure, and then use it as a heat sink with which to lower the temperature and pressure of the bulk of the propellant in the tank. Liquid may also be

circulated within the tank to enhance the cooling processes and to remove any vapor that may have been generated on the walls by boiling. The anticipated heat fluxes at the walls are relatively low, and the flow rates should be optimized to minimize the volume and weight of the circulation equipment. Under such conditions, the absence of buoyancy could be important in determining the forced-convection boiling heat-transfer processes.

A review of the work done on the effects of gravity on forced-convection boiling is provided by Papell in reference 3. It is apparent that the amount of work done in this area is meager and that the work done in the past has been confined to high heat fluxes near burnout and the film boiling regime. Recent work (refs. 4 and 5) done in a drop tower has also been confined to high heat fluxes. The complete lack of information in the low heat flux region, then, makes it an attractive subject area to investigate.

This report presents the results of research conducted in the NASA Lewis Research Center Drop Tower Facility on the effects of gravity on forced-convection boiling at low heat flux. High-speed motion pictures were taken of boiling from a flat-plate heater in water for heat fluxes just above the inception point. The water was slightly subcooled (0.4 to 1.5^{o} C), and the free-stream velocities were of the same order of magnitude as free-convection velocities for the system in normal gravity (4.2 to 11.5 cm/sec).

SYMBOLS

A	heater surface area, cm^2
D	bubble diameter, cm
g_0	Earth gravity, m/sec^2
k	thermal conductivity, W/(m)(K)
Pr	Prandtl number
Q	total heat flux, W
q	heat flux per unit surface area of bubble, W/m^2
R	radial position, cm
T	temperature, K
t	time, sec
U	velocity, cm/sec
$\bar{x}$	axial displacement along surface, cm
Y	vertical distance above heater, cm
δ	boundary layer thickness, cm

θ contact angle, rad

ν kinematic viscosity, m^2/sec

μ dynamic viscosity, kg/(m)(sec)

ρ density, kg/m^3

φ angular position, rad

Subscripts:

b bubble base

e equilibrium

H hydrodynamic conditions

O thermal entrance region

sat saturation conditions

T thermal conditions

w conditions at Y = 0

∞ free-stream conditions

APPARATUS AND PROCEDURE

Drop Tower Facility

The zero-gravity experiment results were obtained in the drop tower shown in figure 1. A test time of 2.2 seconds was obtained by allowing the experiment package to undergo an approximate 23-meter unguided free-fall. The experiment was prepared on the fifth floor of the tower, hoisted to the eighth floor, and suspended from the ceiling by a highly stressed music wire. Release of the experiment was accomplished by pressurization of an air cylinder that forced a knife edge into the support wire, which rested against an anvil. The experiment package was decelerated by allowing aluminum spikes that were mounted on the package to embed in a container filled with sand.

Drag Shield

Air resistance on the experiment package was reduced by allowing the experiment to free-fall inside a protective air-drag shield, as shown in figure 2. The drag shield was designed with a high ratio of weight to frontal area and a low drag coefficient, so

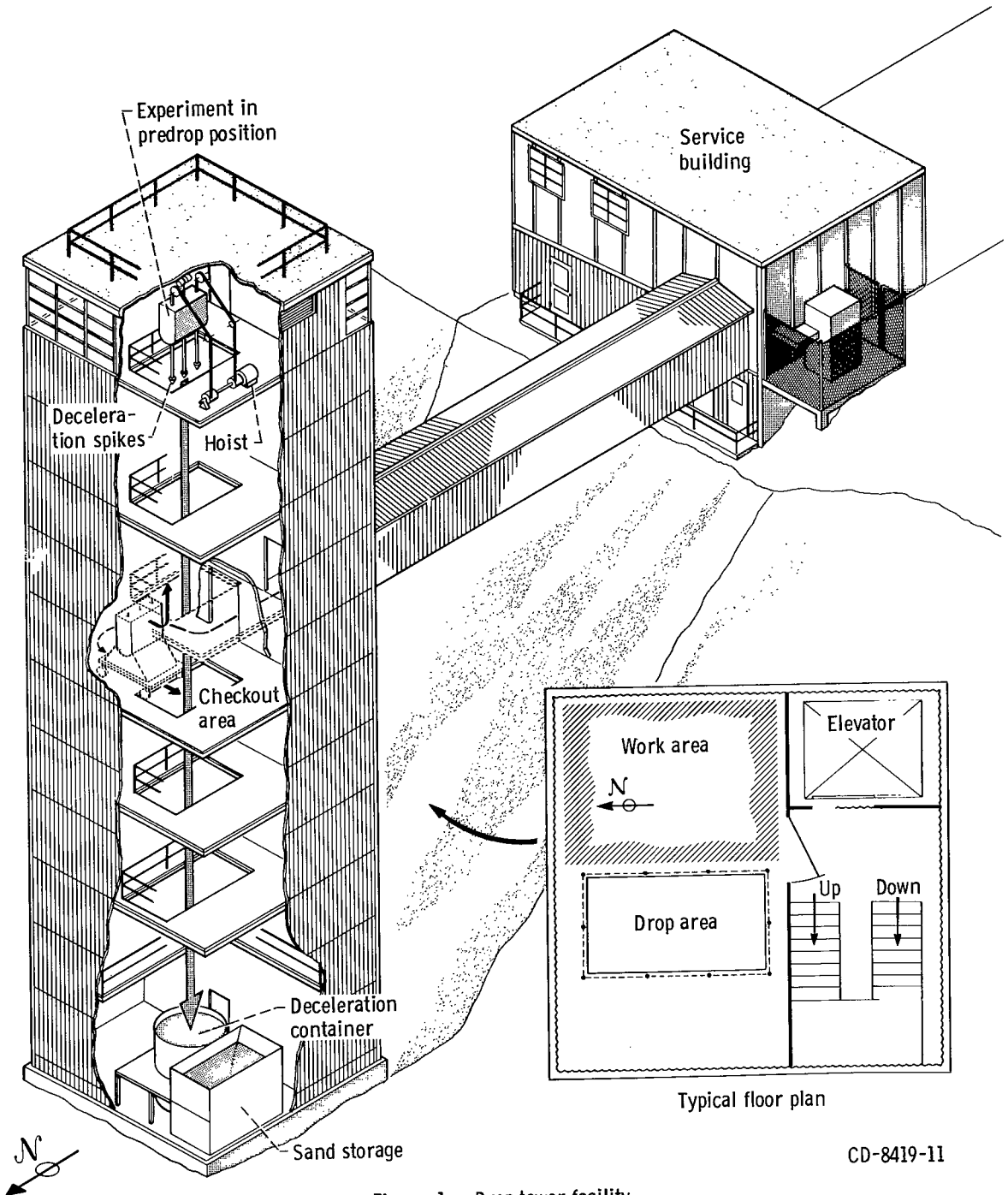

Figure 1. - Drop tower facility.

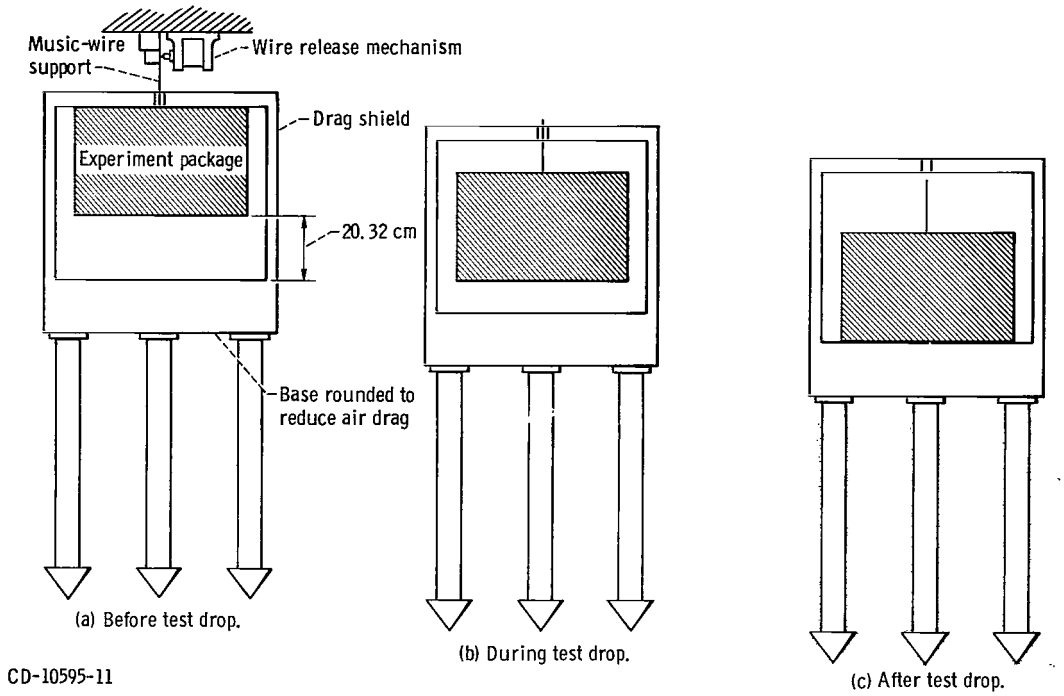

Figure 2. - Schematic drawing showing position of experiment package and drag shield before, during, and after test drop.

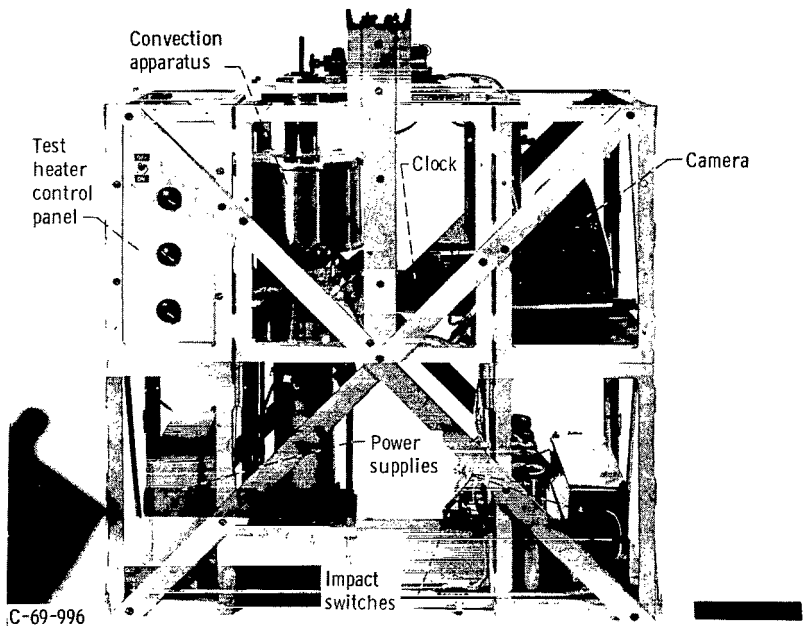

Figure 3. - Experiment package.

that the deviation from true free-fall would be minimized. As a result, the experiment package was subjected to a gravity level of less than 10^{-5} g_0 ($\approx$0). Prior to deceleration in the sand box, the package came to rest on the bottom of the drag shield, which resulted in a usable zero-gravity test time of 2.2 seconds.

Experiment Package

The experiment package, as shown in figure 3, contained the convection apparatus, camera and lighting equipment, clock, power supplies, and associated controls.

A schematic drawing of the convection apparatus is shown in figure 4. It consisted of a motor and power train assembly that drove a piston at a constant speed in a brass

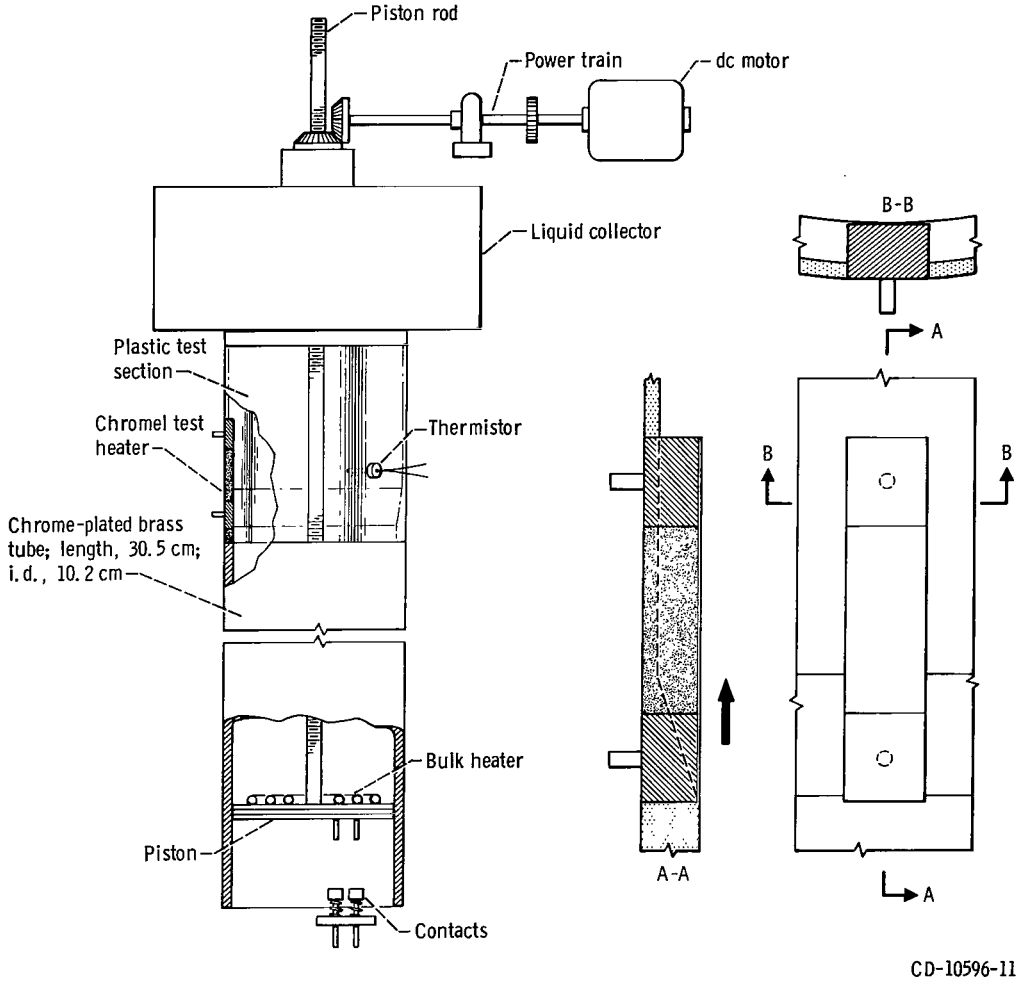

Figure 4. - Convection apparatus.

tube. Adjacent to the brass tube was a plastic section that, in turn, was connected to a liquid collection tank. When operated, the piston started from the lowest position and forced the test liquid at a constant rate upward into the collection tank. A scale was mounted on the piston rod and used to determine the piston speed. The brass tube was wrapped with asbestos insulation to minimize heat losses.

The surface on which boiling was observed was a thin Chromel strip with an effective heating surface of 1.27 by 4.06 centimeters. The underside of the strip was mounted on an insulating material with high-temperature epoxy resin, whereas the ends of the strip were attached with machine screws to copper blocks. The heads of the screws were machined off, and the entire surface was lapped smooth with emery paper. As shown in figure 4, this heater assembly was mounted in the plastic section so that the plane of the heater was tangent to the inside diameter of the section at the leading edge of the assembly. Downstream of this leading edge, the inside diameter of the plastic section slowly increased so that the heater assembly, eventually, was surrounded on three sides by the test liquid. This geometry was chosen to simulate flow over a flat plate and to minimize excessive boiling on the heater edges. Power to the test heater was provided by a 5.5-volt, 64-ampere-hour regulated power supply.

A second heater was mounted on the top face of the piston and used to preheat and deaerate the bulk of the fluid. Alternating-current power to this heater was supplied through a set of spring-loaded contacts when the piston was in the lowest position.

The bulk fluid temperature was measured by a thermistor mounted on the end of a stainless-steel probe that extended about 2.5 centimeters into the flow. Its resistance was read out continuously on a digital ohmmeter prior to dropping.

Heat flux from the heater strip was determined by measuring the voltage drop across the surface with a vacuum-tube voltmeter. The resistance of the strip was measured accurately prior to testing with a Kelvin bridge.

A 16-millimeter motion picture camera, running at a nominal rate of 900 frames per second, filmed the entire heater assembly. Also in the field of view was a digital clock that was accurate to 0.01 second. Illumination was provided by spotlights and aided by reflection from one-half of the plastic test section which was painted white.

Experimental Procedure and Data Reduction

The convection apparatus was cleaned, flushed with alcohol, and filled with distilled water. The experiment package was placed in the drag shield and raised to the top of the tower. Power was applied to the bulk heater to heat the water to the boiling point and to deaerate it. This procedure normally required about $1\frac{1}{2}$ hours.

After the degassing processes were complete, the bulk heater was turned off. The test heater was then actuated at a level that just initiated boiling and the processes were

permitted to come to steady state. The latter condition was evidenced by the regular production of bubbles at the four or five active sites. The experiment package was released after the bulk temperature was recorded.

Prior to the drop, the camera, clock, and lights were activated. Approximately 0.6 second after release, the motor was started and forced convection was initiated. This time delay permitted flows caused by natural convection in normal gravity to dissipate. Observations of the small amount of boiling on the edges of the test heaters and of preliminary tests run at higher heat fluxes where there was appreciable bubble separation from the strip indicated that, upon separation in zero gravity, the bubbles did not move along the strip, but, rather, perpendicular to it. The time 0.6 second was chosen, with due consideration given to the time available for zero-gravity forced convection (1.6 sec), as an upper limit to ensure that the inertial effects were small.

The boiling recorded on film was viewed on a motion analyzer. In addition to generally observing the phenomena, measurements of piston speed and bubble size as a function of time were made. Bubble size and position on the heater were obtained by scaling from a photograph of a surface inscribed with a 0.2-square-centimeter grid installed in place on the heater.

RESULTS AND DISCUSSION

Test Conditions

A summary of the test conditions for the different runs is presented in table I. The subcoolings (saturation temperature minus bulk temperature) were all less than 1.5° C, and the heat fluxes generated were in the vicinity of 1150 watts per square meter. It is apparent from table I that free-stream velocity was the primary test variable. A typical plot of piston displacement as a function of time, from which free-stream velocity was obtained, is shown in figure 5. As can be seen, approximately 0.2 second was required for the piston to come to a velocity that it maintained for the remainder of the test.

General Observations

Normal-gravity free-convection boiling. - The bubbles formed on the surface relatively slowly because of the low surface heat fluxes. Some nucleation sites generated bubbles that appeared to be almost stagnant, whereas other sites produced vapor at regular frequent intervals. Upon separation, the bubbles rose vertically along the surface, occasionally merging with others that were still attached to the surface. Under

TABLE I. - TEST CONDITIONS

Test run	Bulk temperature, T, ^{o}C	Saturation temperature, T_{sat}, ^{o}C	Heat flux, q, W/m^2	Free-stream velocity, U_{∞}, cm/sec
1	98.0	98.9	1223	4.2
2	98.3	99.2	1150	11.5
3	98.5	99.5	1254	7.2
4	98.5	99.5	1254	6.7
5	98.0	99.5	1226	6.9
6	98.8	99.5	1261	6.5
7	98.8	99.4	1072	6.0
8	98.8	99.2	1204	10.2
9	98.0	99.1	1239	9.9
10	98.1	99.1	1210	10.1
11	98.0	99.3	1128	7.4
12	98.5	99.3	1012	8.4
13	97.8	99.1	1305	7.8

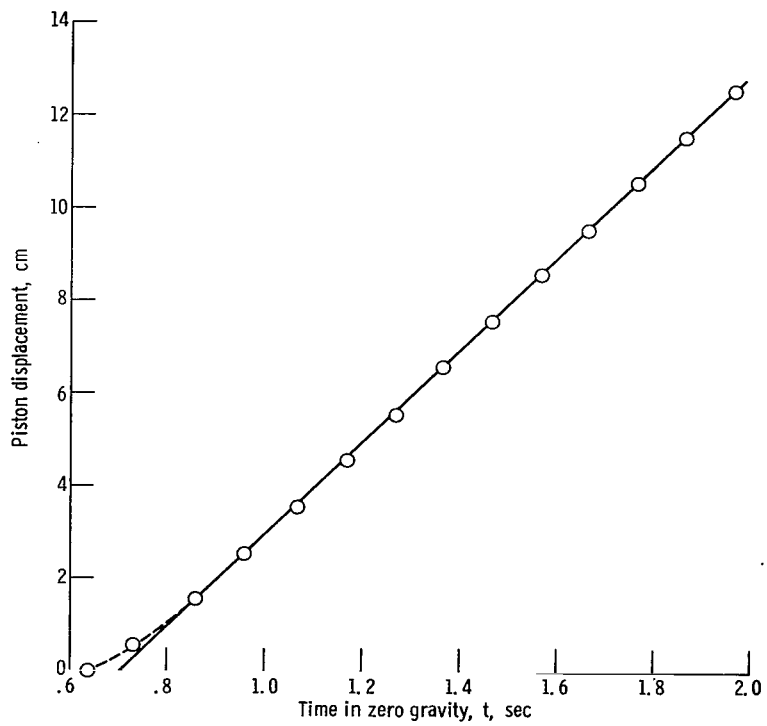

Figure 5. - Piston position as function of time for typical test run.

these test conditions, the dynamics of the attached bubbles would most probably be dominated by buoyant, pressure, inertia, and surface tension forces, whereas the unattached bubbles were dominated by buoyant and drag forces. For a detailed description of the forces and experimental work investigating their importance, see references 6 and 7. The heat-transfer coefficient for the heater surface was mainly determined by the free convection because of the relatively few nucleation sites.

Zero-gravity boiling. - During the zero-gravity portion of the test, prior to forced convection, the bubbles that were on the surface when the experiment package was released remained attached to the surface and increased in size. The latter effect was caused by the dissipation of free convection and subsequent growth of the thermal boundary layer by conduction. Frequently, the bubbles became large enough to coalesce with their neighbors, forming an irregular vapor mass.

Zero-gravity forced-convection boiling. - The behavior of the bubbles after forced convection was started is best described by use of figure 6, which is representative of all the data. Here, bubble diameter, as measured in a plane parallel to the heater surface, is plotted as a function of time in zero gravity for several different free-stream velocities. As can be seen in the figure, the period of time during which the liquid was stagnant and when it was convected is denoted. Further time divisions during forced convection are descriptive of thermal conditions above the surface and are discussed more fully in the appendix.

After the initiation of forced convection, the bubbles continued to grow, reached a maximum, and then decreased in size. They became smaller until a minimum size was reached and, if there was sufficient test time, started to get larger again (figs. 6(c) and (d)). This behavior of the bubbles is an indication of the changing thermal conditions near the heated surface. The irregular bubble growth and collapse at first signifies the removal from the surface of the thermal boundary layer that was present at the start of convection. Collapse of the bubbles at a nearly constant rate indicates that this transient period has ended and that the thermal conditions above the surface were largely determined by the forced-convection process. The fact that the bubbles reached minimum size and then started to increase again characterizes the transient nature of the forced convection. In other words, after the "old" thermal conditions were removed, the "new" thermal boundary layer began with some minimum thickness and increased with time. When the boundary layer reached a size such that the evaporation into the bubbles through this layer and the evaporation from beneath the bubbles just equaled the condensation through the top of the bubbles, a minimum size or thermal equilibrium condition was reached. Subsequent bubble growth then, of course, shows that the thermal boundary layer was continuing to increase. The foregoing description is typical of all the test runs for bubbles that were in existence when convection was started. A series of photographs from test run 5 showing the collapse and growth of a bubble is presented in figure 7.

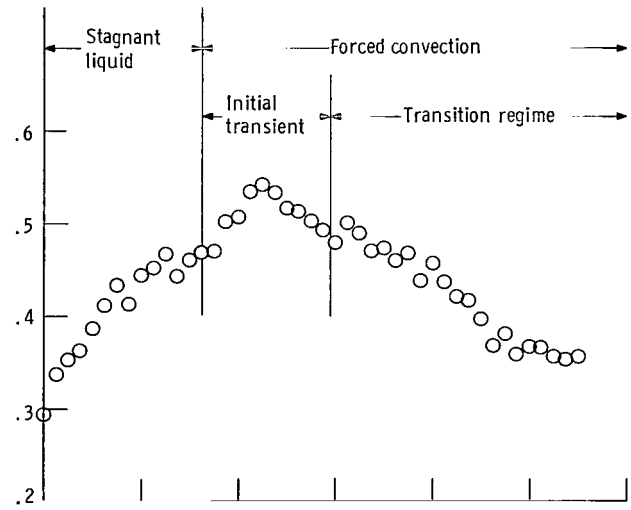

(a) Test run 1. Free-stream velocity, 4.2 centimeters per second.

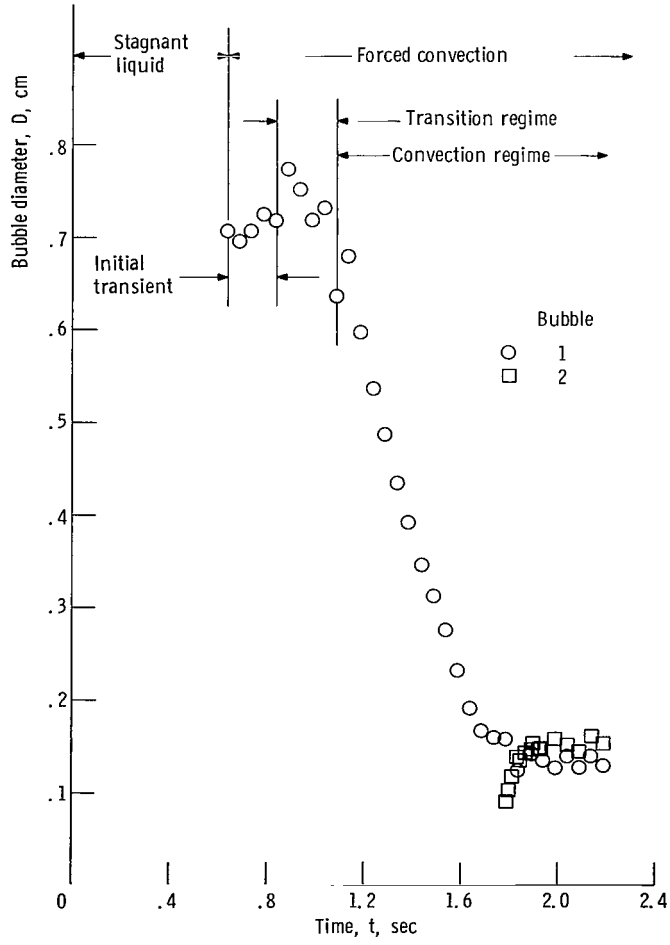

(b) Test run 2. Free-stream velocity, 11.5 centimeters per second.

Figure 6. - Bubble diameter as function of time for various free-stream velocities.

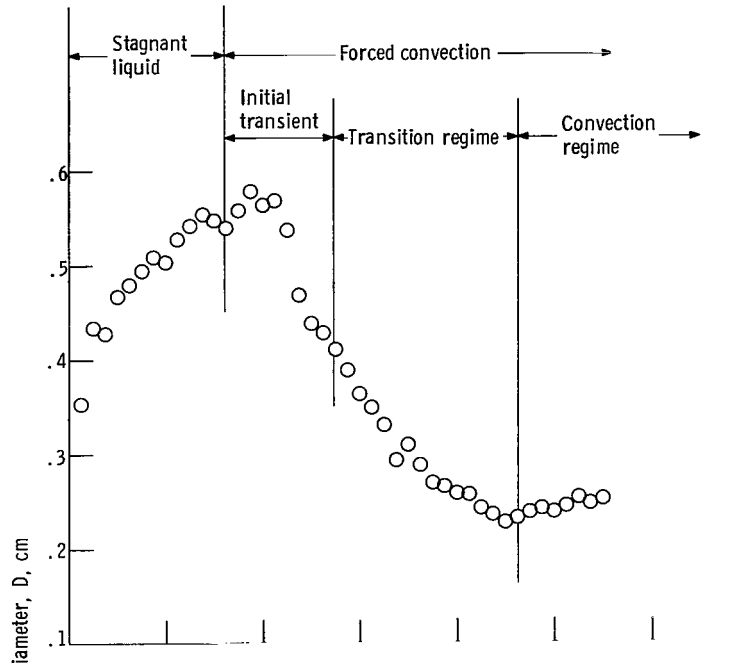

(c) Test run 5. Free-stream velocity, 6.9 centimeters per second.

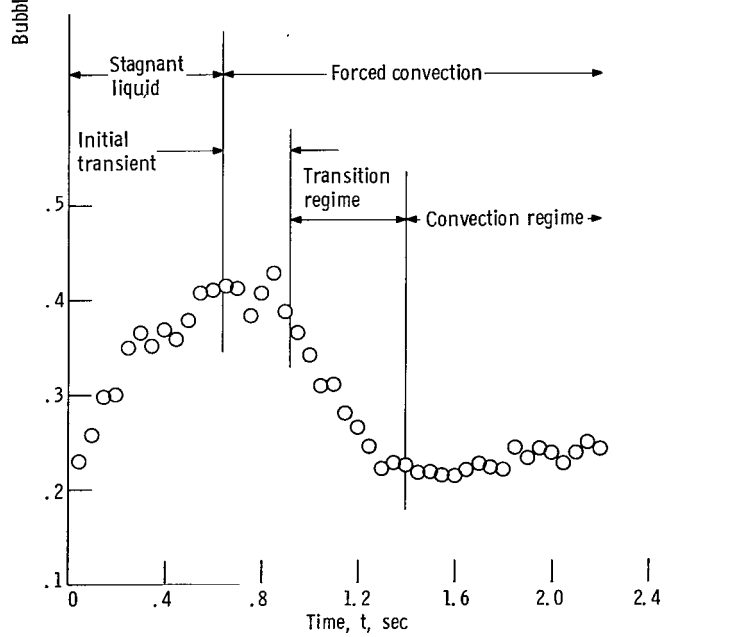

(d) Test run 8. Free-stream velocity, 10.2 centimeters per second.

Figure 6. - Concluded.

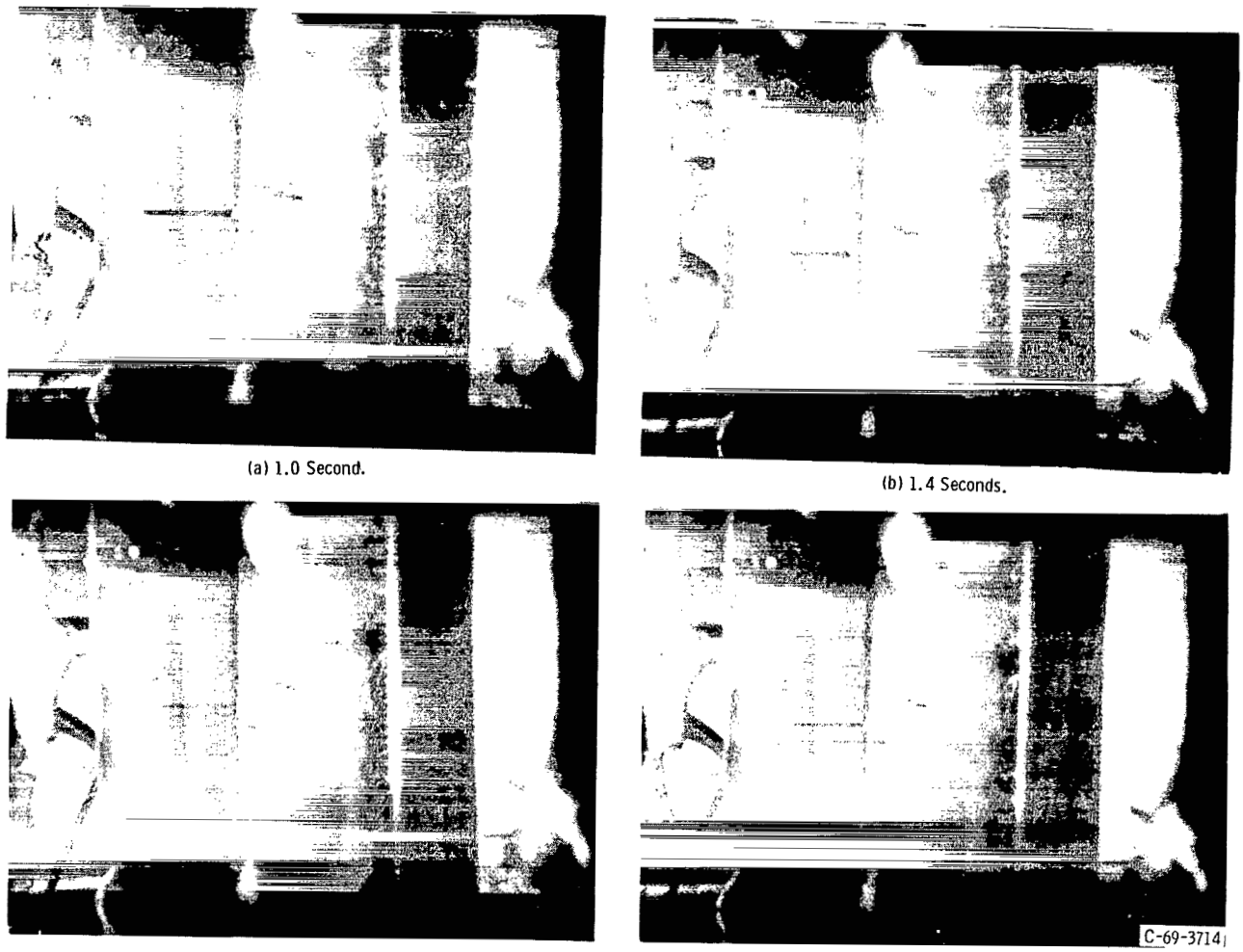

(a) 1.0 Second.

(b) 1.4 Seconds.

(c) 1.8 Seconds.

(d) 2.2 Seconds.

Figure 7. - Growth and collapse of bubble for run 5.

A significant number of new bubbles was generated after forced convection started. Some came from newly activated sites while others formed at sites that, at the start of convection, were under relatively large bubbles. The forced convection, as was just described, decreased the size of the bubbles and, thus, potential nucleation cavities primed with vapor were exposed. The growth characteristics of a newly generated bubble are shown in figure 6(b) for bubble 2.

The vast majority of the bubbles (about 85 percent) remained attached to the surface forming what may be described as a bubble boundary layer. This condition is peculiar to zero gravity since observed normal-gravity boiling (see Normal-gravity free-convection boiling), which had free-convection velocities that were of the same order of magnitude as the imposed forced-convection velocities, showed that the bubbles always separated. The existence of this layer of bubbles is of importance to pro-

pellant tank designers because of their concern with net vapor generation and, hence, the pressure rise characteristics of a sealed tank.

Thermal Equilibrium Bubble Analysis

It was apparent from the experimental data that, for conditions of low heat flux and low flow rates in zero gravity, a layer of bubbles exists adjacent to a heated surface. The films also showed that the size of bubbles on the surface was strongly dependent on the thermal conditions above the surface. Of particular interest is the minimum or thermal equilibrium size D_e that the collapsing and growing bubbles attained. This bubble growth, together with the fact that the thermal conditions on the surface were changing, suggests that a particular set of thermal and hydrodynamic conditions is associated with each bubble size. The processes occurring in this experiment are transient, as evidenced by the fact that the bubbles always changed. However, for steady-state conditions, in which the thermal and hydrodynamic conditions at a particular position are constant, the bubbles on the surface would be constant in size and in

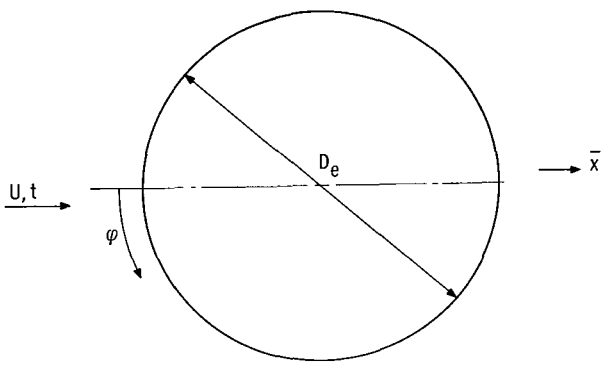

(a) Top view.

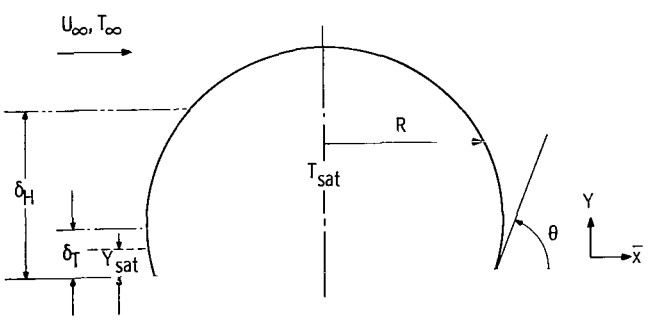

(b) Side view.

Figure 8. - Bubble model.

thermal equilibrium.

The problem to be considered is that of a stagnant bubble on a heated surface in a steady flow field. Such a bubble protruding out of a hydrodynamic layer δ_H and a thermal layer δ_T is depicted in figure 8. Also shown is the evaporation layer thickness Y_{sat}, which is that distance over which the temperature decreases from that at the heater to the saturation temperature. Chao (ref. 8) indicates that the heat transfer per unit area at the bubble liquid-vapor interface in a flow field may be expressed as

$$q = f(\text{fluid properties},\ U,\ T,\ T_{sat},\ R,\ \varphi) \tag{1}$$

where U is the velocity in the vicinity of the interface, T is the temperature away from the bubble interface, T_{sat} is the saturation temperature, R is the radial position, φ is the angular position, and the fluid properties are density, specific heat, thermal conductivity, and viscosity.

To the author's knowledge, a solution for the velocity fields surrounding a bubble attached to a surface and in a hydrodynamic layer is not available. Through logic, however, the basic parameters that the heat flux at the bubble surface is dependent on can be obtained. Assume that

$$U = f(\text{fluid properties},\ U_\infty,\ \delta_H,\ Y,\ \varphi) \tag{2}$$

where U_∞ is the free-stream velocity, and that

$$T = f\left(\text{fluid properties},\ T_\infty,\ \frac{Q_w}{A},\ \delta_T,\ Y\right) \tag{3}$$

where T_∞ is the free-stream temperature and Q_w/A is the constant surface heat flux, and that

$$R = f(D_e,\ \theta,\ Y) \tag{4}$$

where θ is the contact angle and the bubble is symmetric about the Y-axis. Insertion of equations (2) to (4) into (1) and integration over a prescribed surface gives the total heat flux through that surface. For example, the heat flux into the bubble through the evaporation layer thickness may be expressed as

$$Q = f\left(\text{fluid properties},\ U_\infty,\ T_\infty,\ T_{sat},\ \frac{Q_w}{A},\ D_e,\ \theta,\ Y_{sat},\ \delta_H,\ \delta_T\right) \tag{5}$$

Relations for the heat fluxes over the remainder of the bubble surface indicate similar functional dependences.

In the steady-state bubble boundary layer, a bubble is in thermal equilibrium on the surface so that the net heat transfer into a bubble is zero. After the incoming heat is equated to that which is being transferred out, the bubble equilibrium diameter may be expressed as

$$D_e = f\left(\text{fluid properties},\ U_\infty,\ T_\infty,\ T_{sat},\ \frac{Q_w}{A},\ \theta,\ Y_{sat},\ \delta_H,\ \delta_T,\ Q_b\right) \tag{6}$$

where Q_b is the heat transferred through the base of the bubble and is equal to Q_w/A. Since δ_T may be expressed as

$$\delta_T = \left(\text{fluid properties},\ T_\infty,\ T_{sat},\ Y_{sat},\ \frac{Q_w}{A}\right) \tag{7}$$

equation (6) may be reduced to

$$D_e = f\left(\text{fluid properties},\ U_\infty,\ T_\infty,\ T_{sat},\ \frac{Q_w}{A},\ \theta,\ Y_{sat},\ \delta_H\right) \tag{8}$$

Equation (8) then presents the explicit parameters that, in general, determine bubble size. However, the variation in bubble size for a particular fluid of specific subcooling flowing over a surface generating heat at a set rate may be expressed more simply as

$$D_e = f(U_\infty,\ Y_{sat},\ \delta_H) \tag{9}$$

Bubble Boundary Layer Results

The validity of equation (9) may be tested with the data if bubble size as a function of thermal and hydrodynamic conditions for steady state is assumed to be the same as the minimum size the bubbles attained in this experiment. Therefore, for the experiment, the thermal and hydrodynamic conditions as a function of time must be known. Free-stream velocity is a measured variable; however, the hydrodynamic layer thickness and the saturation layer thickness must be calculated. A solution for the conditions on a flat plate pulsed with constant heat flux and over which liquid is impulsively moved is presented in reference 9. The applicability of the experimental test conditions to the problem solved in reference 9 and the equations used to calculate δ_H and Y_{sat} are presented in the appendix.

The results of plotting D_e as a function of the three obtainable correlating parameters, U_∞, δ_H, and Y_{sat}, are presented in figures 9 to 11, respectively. Apparent from figures 9 and 10 is that, although there is some trend in the data, δ_H and U_∞ played a minor role in determining bubble size. This is reasoned from the wide scatter in the values of either U_∞ or δ_H for a particular bubble diameter. Figure 11, however, indicates an apparent linear dependence of bubble diameter on the saturation layer thickness. Doubling the saturation layer thickness resulted in more than a twofold increase in bubble size. It is evident, therefore, that the bubbles were strongly influenced by the thermal conditions close to the heater surface.

Snyder (ref. 10) conducted forced-convection boiling studies at relatively high subcoolings and flow rates as opposed to the low values in this work. A primary conclusion of his work was that the thermal boundary layer had little affect on the bubbles. In light of the difference in test conditions, this result does not contradict the data herein, but, rather, suggests the complicated nature of the explicit form of equation (8).

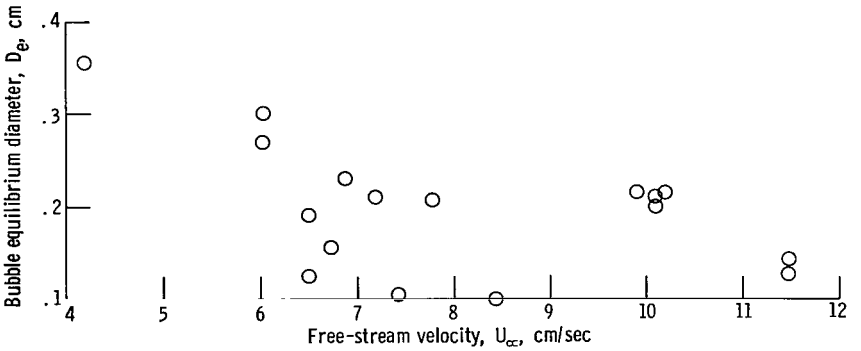

Figure 9. - Bubble diameter as function of free-stream velocity.

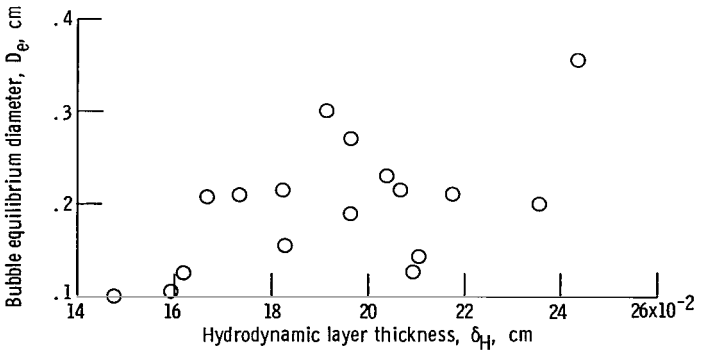

Figure 10. - Bubble diameter as function of hydrodynamic layer thickness.

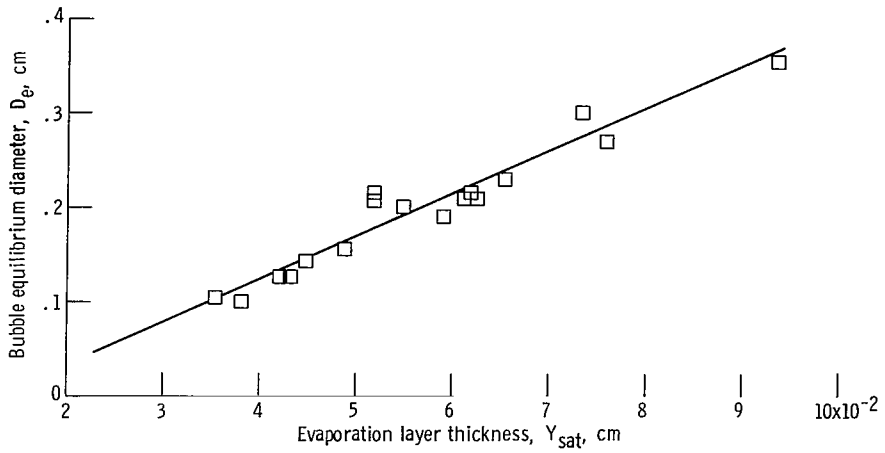

Figure 11. - Bubble diameter as function of evaporation layer thickness.

A correlation for bubble diameter as a function of the saturation layer thickness was determined by assuming a linear relation and by using the method of least squares to fit a curve to the data in figure 11. The result is

$$D_e = -0.06 + 4.6\ Y_{sat} \tag{10}$$

Of interest is that Frost in reference 11 predicted a linear relation between Y_{sat} and D_e, but for bubbles at inception.

CONCLUDING REMARKS

The objective of this research was to investigate a phase of forced-convection boiling that may be applicable to a thermal conditioning system operating in a rocket propellant tank in a zero-gravity environment. In defining the test conditions, it was decided to look at a worst possible case, that is, low subcooling and low flow velocity. Relatively high values of these parameters should present no problems, as the generated vapor either separates from the tank wall and is removed by the flowing liquid or condenses before separation. However, both the subcooling and the flow velocity should be kept as small as possible to optimize design. It is at these low values that gravity has a strong effect on the heat-transfer processes.

The results of the experimentation in zero gravity indicate that at low heat fluxes, typical of what is anticipated at a tank wall, bubbles remain on the surface to form what may be described as a bubble boundary layer. The existence of this layer would be important during the coast phase of a mission because of the increased pressurization of the tank. Consideration must also be given to any effect these bubbles would have on

reorientation maneuvers and propellant outflow.

An analysis was conducted to determine the variables that fixed the size of the bubbles in the boundary layer. This analysis together with the experimental data indicated that, for the test conditions considered, the change in bubble size along a surface was a linear function of the saturation layer thickness Y_{sat} (the distance from the surface at which the liquid temperature equals the saturation temperature). This result not only gives the propellant tank designer a parameter to work with but is also significant from a basic research standpoint. It means that the bubbles on a heated surface in a hydrodynamic boundary layer may be significantly affected by the heat transferred through the saturation layer thickness.

The size D_e of steam bubbles generated on a Chromel surface at low heat flux (near the inception point of boiling) and at low flow velocities (4.2 to 11.5 cm/sec) for slightly subcoolined conditions (1.5° C or less) was successfully correlated in terms of the evaporation layer thickness. The resulting empirical equation is

$$D_e = -0.06 + 4.6\ Y_{sat}$$

Lewis Research Center,
National Aeronautics and Space Administration,
Cleveland, Ohio, October 6, 1969,
124-09.

APPENDIX - HYDRODYNAMIC AND THERMAL CHARACTERISTICS

The situation to be considered is that of a flat plate generating heat at a constant rate and over which liquid is impulsively moved. Reference 9 presents a solution to this problem. The basic assumptions made in the analysis of reference 9 are laminar flow, constant free-stream velocity and temperature, an unheated entrance length, transient hydrodynamic conditions, a step increase in free-stream velocity, and a surface heat flux that is constant and pulsed at zero time. The applicability of the experimental test conditions to these assumptions requires discussion.

Hydrodynamic Conditions

The overall flow in the circular section was analogous to flow in the entrance region of a pipe. Schlichting (ref. 12) indicates that, for small distances from the pipe inlet, the flow may be considered the same as that on a flat plate at zero incidence. The critical Reynolds number $\delta U_\infty \bar{x}/\mu$ for the transition from laminar to turbulent flow on a flat plate is 3.2×10^5. Therefore, a maximum experimental Reynolds number (the position $\bar{x}$ was based on the maximum displacement of fluid particles) of 3.6×10^4 indicates that a laminar flow assumption is indeed valid. The hydrodynamic boundary layer for impulsive laminar flow on a flat plate, from reference 9, is

$$\delta_H = 3.65\sqrt{\nu t} \tag{11}$$

There was not a constant free-stream velocity in the tube. Continuity together with the growth of the hydrodynamic boundary layer required that the free-stream velocity be greater than the piston velocity at positions away from the piston face. However, analysis indicated that the approximate increase for the maximum expected hydrodynamic layer thickness was less than $3\frac{1}{2}$ percent of the piston velocity.

As was shown in figure 5, the piston required some finite time before it came to a constant velocity. A time correction was determined for each test to account for the discrepancy between this condition and the step increase that is assumed in the analysis. This determination was made by extending the constant velocity line on the position-time plot (see fig. 5) to zero displacement and assuming that the liquid particles were behaving as if they had been set in motion at this new time. The resulting time corrections ranged from 0 to 0.08 second.

Thermal Conditions

The analysis considers the heater to be in thermal equilibrium with the liquid prior to the start of forced convection, while actually, a thermal boundary layer existed on the surface in the experiment. Therefore, some time was required before the theoretically predicted conditions could be assumed to approximate the actual ones. Initially, the forced convection decreased the size of the thermal layer to some minimum, and then the boundary layer increased again. The minimum signifies that time when, for a particular displacement along the heated surface, convection as a mode of heat transfer no longer decreased the thermal layer, and the temperature profiles were being defined by conduction from the heated surface. The analysis of reference 9 predicts the time when convection just starts to affect the growth of the thermal layer:

$$\bar{x} - \bar{x}_0 = \left[\frac{3.507}{(Pr)^{1/2}} + \frac{2.687}{(Pr)^{3/2}} - \frac{0.587}{(Pr)^2} - \frac{4.608}{Pr}\right] U_\infty t \tag{12}$$

The notation here is consistent with that in reference 9. These criteria are used to define the initial transient and are shown in the representative data of figure 6. The agreement between the predicted end of the initial transient and when the bubbles start to collapse at a regular rate is, in general, good.

Beyond the initial transient, the thermal conditions may be calculated from the results in reference 9. Provided that enough time exists, two regimes are descriptive of the temperature fields above the surface. Immediately after the initial transient is the transition regime in which the temperature profiles may be approximated from

$$T - T_\infty = 0.625 \frac{Q_w \delta_T}{Ak} \text{ierfc}\left(1.6 \frac{Y}{\delta_T}\right) \tag{13}$$

where

$$\delta_T = 3.2\left(\frac{\nu t}{Pr}\right)^{1/2} \tag{14}$$

The end of this regime is defined by

$$\bar{x} - \bar{x}_0 = \left[\frac{0.443}{(Pr)^{1/2}}\right] U_\infty t \tag{15}$$

Following this regime is the convection regime in which the temperature profile may be

presented as

$$T - T_\infty = \frac{Q_w}{Ak}\left(\frac{\delta_T}{2} - Y + \frac{Y^3}{\delta_T^2} - \frac{Y^4}{2\delta_T^3}\right) \tag{16}$$

where

$$\delta_T = 2.2\left[\frac{\delta_H \nu(\bar{x} - \bar{x}_0)}{U_\infty Pr}\right]^{1/3} \tag{17}$$

Reference 9 contains the descriptions of the regimes together with the justifications for the applicability of the equations. The saturation layer thickness is obtained from equation (13) or (16) by setting T equal to T_{sat} and Y equal to Y_{sat}.

REFERENCES

1. Aydelott, John C.: Effect of Gravity on Self-Pressurization of Spherical Liquid-Hydrogen Tankage. NASA TN D-4286, 1967.

2. Sterbentz, W. H.: Liquid Propellant Thermal Conditioning System. Rep. LMSC-A839783, Lockheed Missiles and Space Co. (NASA CR-72113), Apr. 20, 1967.

3. Papell, S. S.: Buoyancy Effects on Forced-Convective Boiling. Paper 67-HT-63, ASME, Aug. 1967.

4. Ul'ianov, A. F.; and Alad'ev, I. T.: Experimental Study of Heat Transfer During Boiling in Conduits During Weightlessness. Cosmic Res., vol. 6, no. 2, Mar.-Apr. 1968, pp. 217-222.

5. Surak, Anatol: Zero-Gravity Effects on Boiling Heat Transfer and the Critical Heat Flux. Foreign Sci. Bull., vol. 4, no. 10, Oct. 1968, pp. 1-14.

6. Cochran, Thomas H.; Aydelott, John C.; and Spuckler, Charles M.: Experimental Investigation of Nucleate Boiling Bubble Dynamics in Normal and Zero Gravities. NASA TN D-4301, 1968.

7. Siegel, Robert: Effects of Reduced Gravity on Heat Transfer. Advances in Heat Transfer. Vol. 4. J. P. Hartnett and T. F. Irvine, Jr., eds., Academic Press, Inc., 1967, pp. 143-228.

8. Chao, B. T.: Transient Heat and Mass Transfer to a Translating Droplet. J. Heat Transfer, vol. 91, no. 2, May 1969, pp. 273-281.

9. Cochran, Thomas H.; and Jun, Eva T.: Impulsive Motion on a Flat Plate Pulsed with Uniform Heat Flux. NASA TN D-5249, 1969.

10. Snyder, N. W.; and Robin, T. T.: Mass-Transfer Model in Subcooled Nucleate Boiling. Paper 68-HT-51, ASME, Aug. 1968.

11. Frost, W.; and Szakowic, G. S.: An Extension of the Method for Predicting Incipient Boiling on Commercially Finished Surfaces. Paper 67-HT-61, ASME, Aug. 1967.

12. Schlichting, Hermann: Boundary Layer Theory. Fourth ed., McGraw-Hill Book Co., Inc., 1960.